Low Loss LTCC Cavity Filters Using System-on-Package Technology at 60 GHz

Jong-Hoon Lee, *Student Member, IEEE*, Stephane Pinel, *Member, IEEE*, John Papapolymerou, *Senior Member, IEEE*, Joy Laskar, *Senior Member, IEEE* and Manos M. Tentzeris, *Senior Member, IEEE.*

***Abstract* – In this paper, three-dimensional (3-D) integrated cavity resonators and filters consisting of via walls are demonstrated, as a system-on-package (SOP) compact solution for RF front-end modules at 60 GHz using the low-temperature cofired ceramic (LTCC) technology. Slot excitation with a $\lambda_g/4$ open stub has been applied and evaluated in terms of experimental performance and fabrication accuracy and simplicity. The strongly coupled cavity resonator provides an insertion loss < 0.84 dB, a return loss >20.6 dB over the pass band (~0.89 GHz) and a 3dB bandwidth of about 1.5 % (~0.89 GHz) as well as a simple fabrication of the feeding structure (since it does not require to drill vias to implement the feeding structure). The design has been utilized to develop a three-dimensional (3-D) low loss 3-pole band pass filter for 60 GHz WLAN narrowband (~ 1GHz) applications. This is the first demonstration entirely authenticated by measurement data for 60 GHz 3-D LTCC cavity filters. This filter exhibits an insertion loss of 2.14 dB at the center frequency of 58.7 GHz, a rejection > 16.4 dB over the passband and a 3-dB bandwidth about 1.38% (~0.9 GHz).**

***Index Terms* –cavity resonators, cavity filters, low-temperature co-fired ceramic (LTCC), band pass filter (BPF), system-on-package (SOP), millimeter-wave (mmW), three-dimensional (3-D) integration**

I. Introduction

The rapid growth of wireless local area and personal communication networks, as well as sensor applications has led to a dramatic increase of interest in the regimes of RF/microwave/millimeter-wave (mmW) systems [1]. Such emerging applications with data rates in excess of 100 Mb/s require real estate efficiency, low-cost manufacturing, and excellent performance achieved by a high level of integration of embedded functions using low-cost and high-performance materials. The multilayer low-temperature cofired ceramic (LTCC) System-On-Package (SOP) [2] has emerged as a candidate to provide an efficient integration of the RF passives due to its mature multilayer fabrication capability and its relatively low cost [2]. On-package integrated cavity filters using LTCC multilayer technology are a very attractive option for three-dimensional (3-D) RF front-end modules up to the mmW frequency range because of their relatively high quality factor (Q) compared to stripline/microstrip [3-4] or lumped element type filters [5].

Numerous publications [6-15] have dealt with 3-D low-loss and high-Q resonators/band pass filters utilizing electromagnetic band-gap (EBG) substrates and micromachined technology. In particular, the recent development of Duroid-based EBG cavity resonators and filters [6-7] have demonstrated advantages of implementing EBG instead of fully conducting metals [8] as side walls in terms of reconfigurability and inexpensive mass production. The idea of using rows of stacked vias as side walls has been applied to produce high Q_u (over 1000) cavity resonators at Ku band [9] and low loss quasi-planar 2-pole filters based on capacitive loaded cavities at Q band [10] using LTCC technology. Also, narrow-band 2-pole filters, which can be embedded inside packaging, have been implemented in LTCC by employing capacitive loading techniques at X-band [11]. For V-band applications, planar alumina waveguide filters with CPW I/O ports have exhibited low insertion loss (<3dB) and good stop-band rejection but occupy large real estate because of the two-dimensional (2-D) arrangement of the resonators [12-13].

In this paper, we present the first extensive report, entirely validated by measured data on low-loss 60 GHz (V-band) 3-D multilayer cavity resonators and three-pole band pass filters utilizing via fences as side walls, enabling a complete passive solution for 3-D compact, low-cost wireless RF front-end modules in LTCC. The slot excitation with a $\lambda_g/4$ open stub is employed for 60GHz cavity resonators and evaluated in terms of S-parameters, bandwidth and fabrication simplicity based on measurement data. After ensuring the performance of the slot excitation technique at V-band (55GHz – 65 GHz), a compact and low-loss 3-D geometry of 3-pole band pass filters has been implemented by importing three identical cavity resonators coupled together with moderate external and inter-resonator couplings for 60GHz WLAN narrowband (~ 1GHz) applications.

II. Rectangular Cavity resonator

The proposed cavity resonators are based on the theory of rectangular cavity resonators [16] and all designs are optimized with the aid of a FEM-based full-wave simulator (HFSS).

The cavity resonator is built utilizing conducting planes as horizontal walls and via fences as side walls as shown in figure 1. The size (d in Fig. 1) and spacing (p in Fig. 1) of via posts are properly chosen to prevent electromagnetic field leakage and to achieve stop-band characteristic at the desired resonant frequency [6]. The resonant frequency of the TE_{mnl} mode is obtained by [16]

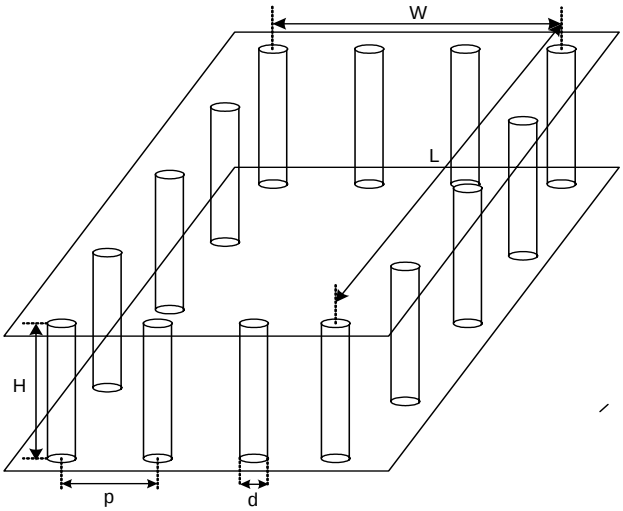

Figure 1. Cavity resonator utilizing via fences as side walls

$$f_{res} = \frac{c}{2\pi\sqrt{\varepsilon_r}}\sqrt{\left(\frac{m\pi}{L}\right)^2 + \left(\frac{n\pi}{H}\right)^2 + \left(\frac{l\pi}{W}\right)^2} \quad (1)$$

where f_{res} is the resonant frequency, c the speed of light, ε_r the dielectric constant, L the length of cavity, W the width of cavity, and H the height of the cavity. Using (1), the initial dimensions of the cavity with perfectly conducting walls are determined for a resonant frequency of 60 GHz for the TE_{101} dominant mode by simply indexing m=1, n=0, l=1 and optimized with a full-wave electromagnetic simulator (L=1.95mm, W=1.275mm, H=0.3mm). Then the design parameters of the feeding structures are slightly modified to achieve the best performance in terms of low insertion loss and accurate resonant frequency. In section III of this paper, we discuss the slot excitation with a $\lambda_g/4$ open stub.

To decrease the metal loss and enhance the quality factor, the vertical conducting walls are replaced by a lattice of via posts. In our case, we used Cassivi's expressions [17] to get the preliminary design values, and then the final dimensions of the cavity are fine tuned with the HFSS simulator. The spacing (p) between the via posts of the sidewalls is limited to less than half guided wavelength ($\lambda_g/2$) at the highest frequency of interest so that the radiation losses becomes negligible [6]. Also, it has been proven that smaller via sizes result in an overall size reduction of the cavity [6]. In our case, we used the minimum size of vias (d (via diameter) = 130 μm in Fig.1) allowed by the LTCC design rules. Also, the spacing between the vias has been set to the minimum via pitch (390μm).

In the case of low external coupling, the unloaded Q, Q_u, is controlled by three loss mechanisms and defined by [18]

$$Q_u = \left(\frac{1}{Q_{cond}} + \frac{1}{Q_{dielec}} + \frac{1}{Q_{rad}}\right)^{-1} \quad (2)$$

where Q_{cond}, Q_{dielec}, and Q_{rad} take into account the conductor loss from the horizontal plates (the metal loss of the horizontal plates dominates especially for a thin substrate such as 0.3mm), the dielectric loss from the filling substrates, and the leakage loss through the via walls, respectively. Since the gap between the via posts is less than $\lambda_g/2$ at the highest frequency of interest as mentioned, the leakage (radiation) loss can be negligible as mentioned above and the individual quantity of two other quality factors can be obtained from [18]

$$Q_{cond} = \frac{(kWL)^3 H\eta}{2\pi^2 R_m (2W^3H + 2L^3H + W^3L + L^3W)} \quad (3)$$

where k is the wave number in the resonator ($(2\pi f_{res}(\varepsilon_r)^{1/2})/c$), R_m is the surface resistance of the cavity ground planes ($(\pi f_{res}\mu/\sigma)^{1/2}$), η is the wave impedance of the LTCC resonator filling, L,W,H the length, width, and height of the cavity resonator, respectively and

$$Q_{dielec} = \frac{1}{\tan(\delta)} \quad (4)$$

where tanδ is the loss tangent (=0.0015) of the LTCC substrate.

All fabricated filters were measured using the Agilent 8510C Network Analyzer and Cascade Microtech probe station with 250 μm pitch air coplanar probes.

III. Cavity Feeding Structure

Figure 2 shows (a) the top view (b) a 3-D overview and (c) the side view of the microstrip-fed cavity resonator using a $\lambda_g/4$ open stub slot excitation technique. Microstrip lines are utilized to excite the resonator through coupling slots etched in the top metal layer (metal 2) of the cavity as shown in figure 2 (c). In order to maximize the magnetic coupling by maximizing magnetic currents, a short is placed at the center of each slot by terminating the feedlines with $\lambda_g/4$ open stubs. The excitation using an open stub contributes to fabrication simplicity with no need to drill via holes to short the end of feedlines. Also, it avoids the loss and inductance effects generated by shorting vias close to the slot, which could be serious in the millimetre-wave frequency range.

The accurate design of the external coupling slots is a key issue to achieve low loss cavity resonators. The external coupling factor is directly related to the input resistance and reactance that can be controlled by the position and size of the coupling aperture [19]. To determine the dimensions of the slots for the optimum response, the coupling slots are initially located at a quarter of the cavity length (SP in Fig. 2 (a)) to maximize the coupling [6], and then the slot width (SW in Fig. 2 (a)) is varied with the constant slot length (SL≈λg/4 in Fig. 2 (a)). The dimensions of the coupling slots have been determined to 0.538 × 0.21 mm^2. The position of the slots is adjusted to obtain the desired insertion loss, resonant frequency and input impedances. The optimized results of resonant frequency, insertion loss, and bandwidth are obtained with SP=0.4475 mm (≈ 0.19λg) (Fig. 2 (a)).

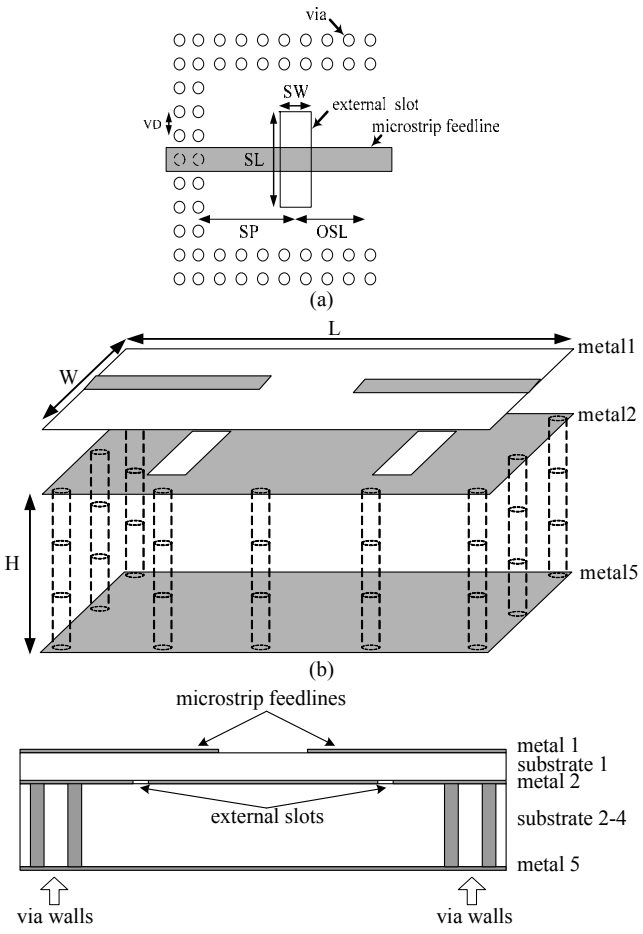

Figure 2. LTCC cavity resonator employing slot excitation with a open stub (a) top view of feeding structure, (b) 3-D overview and (c) sideview of the proposed resonator

The solid conducting sidewalls are replaced with rows of vias. The spacing between via rows is set up to the minimum via pitch (390μm). In this process, major filter characteristics such as resonant frequency and insertion loss are not only affected by the via pitch/diameter but also by the number of rows of vias. The resonator characteristics are investigated with the increase of the number of via rows (1→3). Double and triple rows exhibit almost the same characteristics such as an insertion loss of 1.14 dB, while a single row exhibits 1 dB higher insertion loss due to a higher leakage. Figure 3 shows the electric field distributions inside the cavity surrounded by rows of vias. It is clearly observed that two rows of vias are sufficient to block the field leakage through the vias. All the final design parameters are summarized in Table I.

Although it has been verified that double and triple rows exhibit almost the same performance in simulations, three rows of via posts were used to ensure a high level of leakage block with respect to both the simulation error and the fabrication accuracy.

Once, the slot size/position and cavity size is determined, the length of the open-circuited stub is optimized to maximize the magnetic coupling. The length (OSL in Fig. 2 (a)) of open-circuited stub is initially set up to $\lambda_g/4$. The

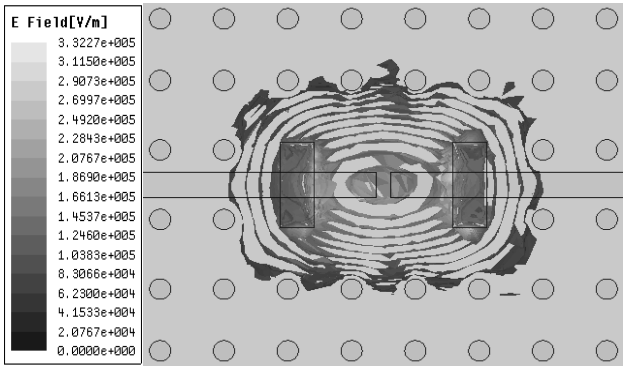

Figure 3. Magnitude of electric field distribution on horizontal plane inside the cavity using slot excitation with an open stub at the resonant frequency (=59.2 GHz)

TABLE I
DESIGN PARAMETERS OF CAVITY RESONATORS USING OPEN STUBS

Design Parameters	***Dimensions (mm)***
cavity length (L)	1.95
cavity width (W)	1.318
cavity height (H)	0.3
slot positioning (SP)	0.4475
open stub length (OSL)	0.485
slot length (SL)	0.538
slot width (SW)	0.21
via pitch (VD)	0.39
via diameter	0.13
via rows	3

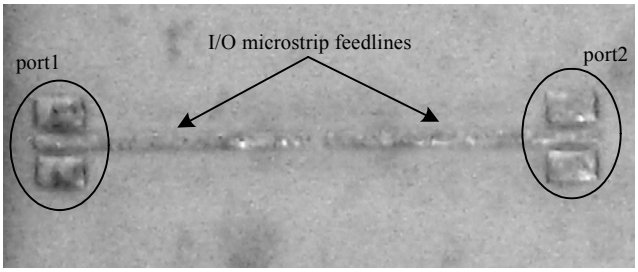

Figure 4. The photograph of the fabricated input/output microstrip feedlines with an open stub and CPW probe pads utilized to excite the embedded the cavity resonator

fringing fields generated by open-end discontinuity can be modelled by an equivalent length of transmission line [22], which is determined to be about $\lambda_g/20$. Therefore, the optimum length of the stub is approximately $\lambda_g/5$ due to the effect of fringing field.

The coupling coefficient between the cavity resonator and the feeding microstrip line can be analytically evaluated using (5). First, Q_{ext} due to the aperture coupling of microstrip feeding is obtained by utilizing Wheeler's equivalent energy concept [20] and parallel-plate waveguide model of microstrip line [21] and then the coupling coefficient is given as [15]

$$k = \frac{Q_u}{Q_{ext}} \tag{5}$$

where k is the coupling coefficient of external coupling and Q_u, the unloaded Q from (2).

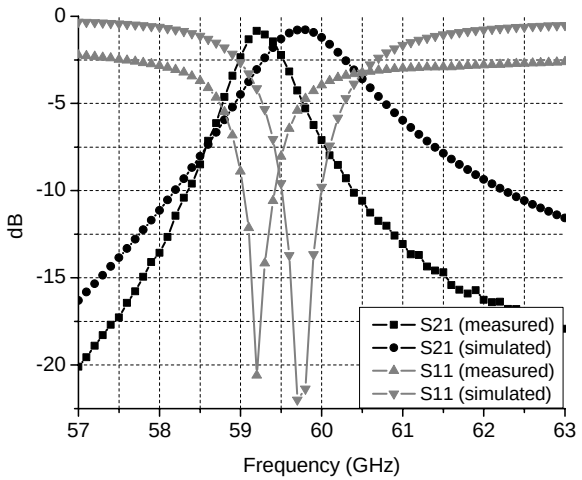

(a)

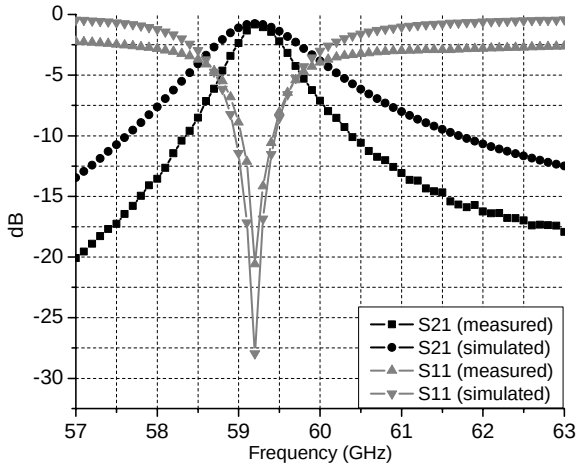

(b)

Figure 5. The comparison between measured and simulated S-parameters (S11 & S21) of 0.3mm-height cavity resonator using slot excitation with an open stub. (a) simulation with $\varepsilon_r = 5.4$ vs. measurement (b) simulation with $\varepsilon_r = 5.5$ vs. measurement.

The proposed cavity resonator was fabricated in an LTCC 044 SiO_2-B2O3 glass by Asahi Glass Co. The relative permittivity (ε_r) of the substrate is 5.4 and its loss tangent (tanδ) is 0.0015 at 35 GHz. The dielectric layer thickness per layer is 100 μm, and the metal thickness is 9 μm. The resistivity of metal (silver trace) is determined to be $2.7\times10^{-8}\Omega\bullet$m. The top view of the microstrip feedlines and CPW probe pads utilized to excite the embedded cavity resonator is shown in figure 4. The overall size is 3.8 mm×3.2 mm×0.3 mm^3 (including the CPW measurement pads).

The measured insertion and reflection loss of the fabricated cavity are compared with the simulated results in figure 5 (a). In the measurement, the capacitance and inductance effects of the probing pads are de-embedded by use of "Wincal" software so that effects, such as those due to the CPW loading become negligible. The cavity exhibits

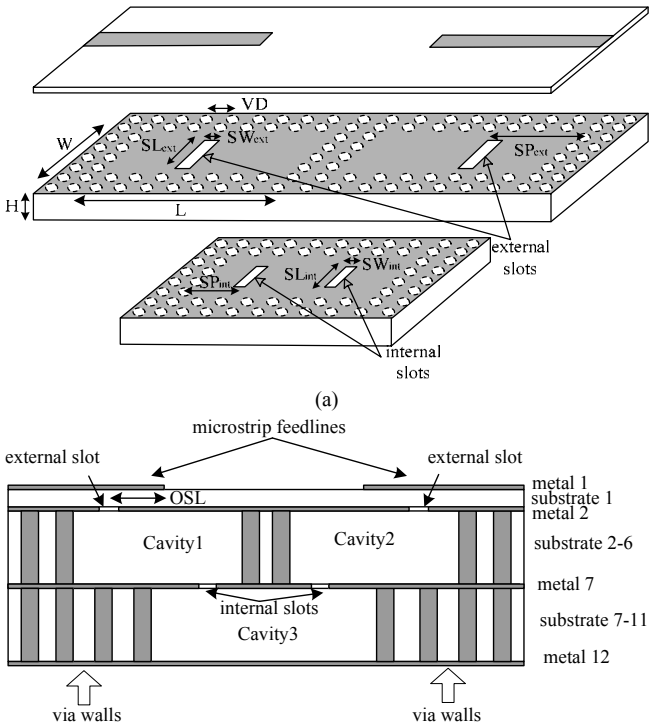

Figure 6. LTCC 3-pole cavity band pass filter employing slot excitation with an open stub: (a) 3-D overview, (b) side view of the proposed filter

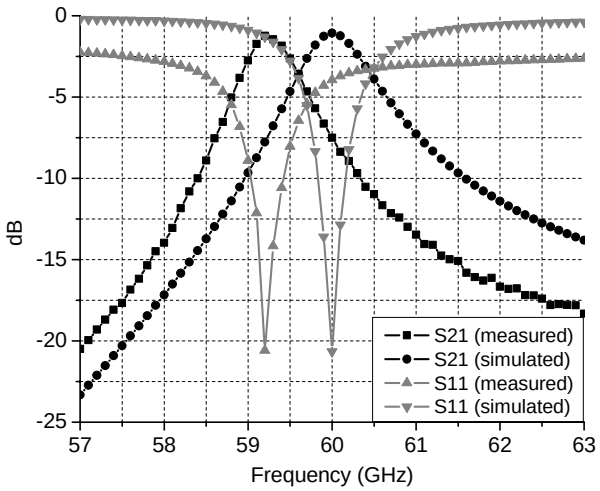

Figure 7. The comparison between measured and simulated S-parameters (S11 & S21) of 0.5mm-height cavity resonator using slot excitation with an open stub.

an insertion loss < 0.84 dB, a return loss >20.6 dB over pass band, and a 3dB bandwidth of about 1.5 % at a center frequency of 59.2 GHz. The simulation results for the insertion loss (<0.78dB) and the return loss (>22dB) correlate well with the experiments but exhibit a slightly increased bandwidth of 2.3% at a center frequency of 59.8 GHz. The center frequency downshift can be attributed to the dielectric constant variation at these high frequencies. The preliminary HFSS simulation presumed that the averaged relative permittivity would be increased to 5.5

across 55-65 GHz. An expanded plot of a comparison of the simulation with ε_r=5.5 and the measurement is shown in figure 5 (b). The coincidence between the center frequencies is observed in figure 5 (b). The narrower bandwidth in measurements might be due to the fabrication accuracy of the slot design that has been optimized for the original resonant frequencies and not for the shifted frequencies.

The Qu can be calculated using the following equations (6)-(8) [6]

$$Q_u = \left(\frac{1}{Q_l} - \frac{1}{Q_{ext}} \right)^{-1} \tag{6}$$

$$Q_l = \frac{f_{res}}{\Delta f} \tag{7}$$

$$S_{21}(dB) = 20\log_{10}\left(\frac{Q_l}{Q_{ext}} \right) \tag{8}$$

where Q_l is loaded Q, and Δf is 3-dB bandwidth. The weak external coupling allows for the apt verification of Q_u of the cavity resonator since Q_u approaches Q_l with the weak external coupling as described in (6). Also the weak coupling abates sensitivity of the measurement on the amplitude of S_{21}. Using the above definitions, a weakly coupled cavity resonator (S21~20dB) has been separately investigated in HFSS and exhibits a Q_u of 367 at 59.8 GHz compared to the theoretical Q_u of 372 at 60 GHz from (2-4).

IV. 3-POLE FILTER

We have designed and fabricated three-pole filters using via walls for 60GHz WLAN narrowband (~ 1GHz) applications that consist of three coupled cavity resonators (Cavity1, Cavity2, Cavity 3 in Fig. 6 (b)). The 3-D overview (a) and side view (b) are illustrated in figure 6. The 3-pole band pass filter based on a Chebyshev lowpass prototype filter is developed for a center frequency of 60 GHz, < 3 dB insertion loss, 0.1 dB in band ripple and 1.67 % fractional bandwidth.

To meet design specifications, the cavity height (H in Fig. 2 (b)) was increased to 0.5 mm (five substrate layers) to achieve a higher Q_u and consequently to obtain narrower bandwidth. The cavity resonator with 0.5mm height has been fabricated in LTCC and measured. The comparison between the simulation and the measurement is shown in figure 7. An insertion loss of 1.24 dB at the center frequency of 59.2 GHz and a narrow bandwidth of 1.35 % (~0.8 GHz) has been measured. The theoretical Q_u yields 426 and it is very close to the simulated Q_u of 424 from a weakly coupled cavity in HFSS.

After verifying the experimental performance of a single cavity resonator, the external coupling and the inter-resonator coupling are considered for the 3-pole filter design.

Firstly, Q_{ext} can be defined from the specifications as follows [22]

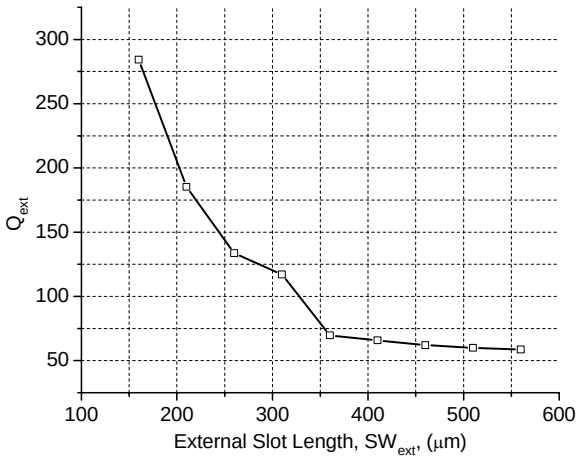

(a)

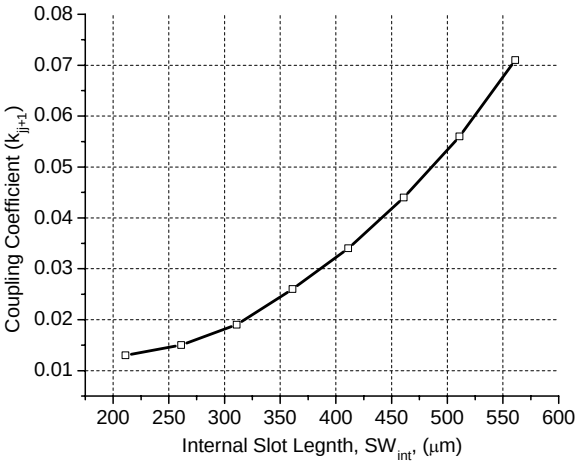

(b)

Figure 8. (a) External quality factor (Q_{ext}) evaluated as a function of external slot width (SW_{ext}) (b) Inter-resonator coupling coefficient (k_{jj+1}), as a function of internal slot width (SW_{int}).

$$Q_{ext} = \frac{g_i g_{i+1} f_{res}}{BW} \tag{9}$$

where g_i are the element values of the low pass prototype, f_{res} is the resonant frequency, and BW is the bandwidth of the filter. The input and output Q_{ext} were calculated to be 61.89. The position and size of the external slots (Fig. 6 (a)) are the main parameters to achieve the desired Q_{ext}. The slots have been positioned at a quarter of the cavity length (L/4) and their length has been fixed to $\lambda_g/4$ ($SL_{ext} \approx \lambda_g/4$ in Fig. 6 (a)). Then, Q_{ext} (shown in Fig. 8 (a)) has been (using full-wave simulations) evaluated as a function of the external slot width (SW_{ext} in Fig. 6 (a)) based on the following relationship [22]

$$Q_{ext} = \frac{f_{res}}{\Delta f_{\pm 90^\circ}} \tag{10}$$

where $\Delta f_{\pm 90^\circ}$ is the frequency difference between ±90° phase response of S11.

Secondly, the inter-resonator coupling coefficients (k_{jj+1}) between the vertically adjacent resonators is determined by

TABLE II
DESIGN PARAMETERS OF 3-POLE CAVITY FILTER USING AN OPEN STUB

Design Parameters	*Dimensions (mm)*
effective cavity resonator (L×W×H)	1.95×1.32×0.5
external slot position (SP_{ext})	0.4125
external slot (SL_{ext}× SW_{ext})	0.46 ×0.538
internal slot position (SP_{int})	0.3915
internal slot (SL_{int}× SW_{int})	0.261×0.4
open stub length (OSL)	0.538
via spacing	0.39
via diameter	0.13
via rows	3

[22]

$$k_{jj+1} = \frac{BW}{f_{res}} \sqrt{\frac{1}{g_j g_{j+1}}} \qquad (11)$$

where j = 1 or 2 because of the symmetrical nature of the filter. k_{jj+1} was calculated to be 0.0153. To extract the desired k_{jj+1}, the size of internal slots (Fig. 6 (a)) is optimized using full wave simulations to find the two characteristic frequencies (f_{c1}, f_{c2}) that are the frequencies of the peaks in the transmission response of the coupled structure when an electric wall or magnetic wall, respectively, is inserted in the symmetrical plane [22]. Then, k_{jj+1} can be determined by measuring the amount that the two characteristic frequencies deviate from the resonant frequency. The relationship between k_{jj+1} and the characteristic frequencies (f_{c1}, f_{c2}) is defined as follows: [22].

$$k_{jj+1} = \frac{f_{c2}^2 - f_{c1}^2}{f_{c2}^2 + f_{c1}^2} \qquad (12)$$

Based on the above theory, the physical dimensions of internal slots were determined by using a simple graphical approach displaying two distinct peaks of character frequencies for a fixed Q_{ext}. Figure 8 (b) shows the graphical relationship between k_{jj+1} and internal slot width (SW_{int} in Fig. 6 (a)) variation with the fixed slot length ($SL_{int} \approx \lambda_g/4$ in Fig. 6 (a)). SW_{int} was determined to be 0.261 mm corresponding to the required k_{jj+1}(≈0.0153) from figure 8 (b). After determining the initial dimensions of the external/internal slots, the other design parameters such as the open stub length (OSL in Fig. 6 (b)) and the cavity length and width (L and W in Fig. 6 (a)) using via walls are determined under the design guidelines described in Section II and III.

The initial dimensions of the external/internal slot widths are set up as optimal variables and fine tuned to achieve the desired frequency response using HFSS simulators. The summary of all design parameters for the 3-pole filter is given in Table II. Figure 9 (a) and (b) show the comparison between the simulated and the measured S-parameters of the bandpass filter. In the measurements, the parasitic

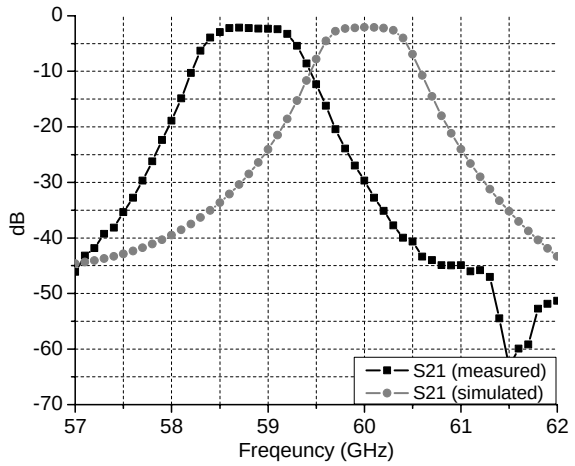

(a)

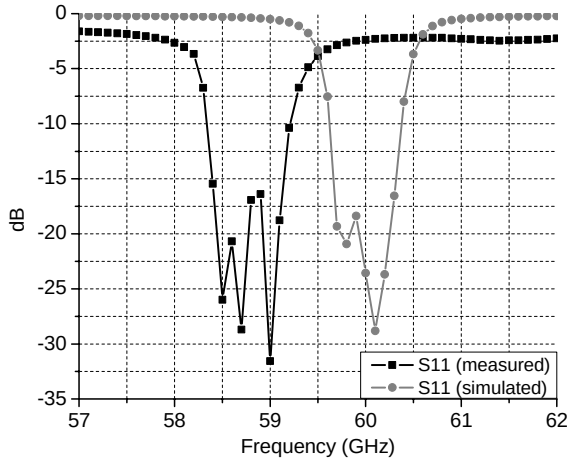

(b)

Figure 9. The comparison between measured and simulated (a) S21 and (b) S11 of 3-pole cavity bandpass filter using slot excitation with an open stub.

effects from the I/O open pads were de-embedded with the aid of WinCal3.0 software. The filter exhibits an insertion loss <2.14 dB which is slightly higher than the simulated value of <2.08 dB, and a return loss > 16.39 dB compared to a simulated value > 18.37 dB over the pass band shown in figure 9 (a) and (b) respectively. In figure 9 (a), the measurement shows a slightly increased 3 dB fractional bandwidth of about 1.53 % (≈0.9 GHz) at a center frequency 58.7 GHz. The simulated results give a 3 dB bandwidth of 1.47 % (≈0.88 GHz) at a center frequency 60 GHz. The center frequency downshift can be attributed to the fabrication accuracy such as slot positioning affected by the alignment between layers, layer thickness tolerance and higher dielectric constant at this high frequency range (55-65GHz) than 5.4 that is the relative permittivity at 35 GHz as mentioned in section III. The overall response of the measurement is in agreement with the simulation except a frequency shift of 1.3 GHz (~2%). This 3-pole filter can be used in the development of 3-pole duplexers for millimeter-wave wireless systems.

V. CONCLUSION

In this work, 3-D integrated cavity resonators and 3-pole filters composed of via walls have been successfully demonstrated with excellent performance using LTCC technology at 60GHz. The slot excitation with a $\lambda_g/4$ open has been studied and the resulting weak-coupling cavity demonstrated excellent performances in terms of a low insertion loss (~0.84 dB) at 59.2 GHz and a 3dB bandwidth of about 1.5 % (~0.89 GHz) as well as fabrication simplicity. A low-loss, fully integrated 3-pole band pass filter employing a slot excitation with an open stub has been implemented for the first time for 60GHz WLAN narrowband (~ 1GHz) applications. It exhibited an insertion loss of 2.14 dB at a center frequency of 58.7 GHz, a return loss $\geq$ 16.39 dB over the passband and a 3-dB fractional bandwidth about 1.38% (~0.9 GHz). To the best of the authors' knowledge, this is the lowest loss reported for a LTCC 3D integrated narrowband filter at 60 GHz. The presented structures can be easily integrated within a 3D LTCC 60GHz front-end module and can also be used in the development of multi-pole 60 GHz duplexers for a system-on-package RF front end.

ACKNOWLEDGEMENT

The authors wish to acknowledge the support of Asahi Glass Co., the Georgia Tech. Packaging Research Center, the Georgia Electronic Design Center, the NSF CAREER Award #ECS-9984761, and the NSF Grant #ECS-0313951.

REFERENCES

[1] H.H.Meinel, "Commercial Applications of Millimeterwaves History, Present Status, and Future Trends," *IEEE Transaction on Microwave Theory and Technique*, Vol. 43, NO. 7, pp. 1639-1653, July 1995.

[2] K.Lim, S.Pinel, M.F.Davis, A.Sutono, C.-H.Lee, D.Heo, A.Obatoynbo, J.Laskar, E.M.Tentzeris, and R.Tummala, "RF-System-On-Package (SOP) for Wireless Communications," *IEEE Microwave Magazine*, Vol.3, No.1, pp.88-99, Mar. 2002.

[3] C.H.Lee, A.Sutono, S.Han, K.Lim, S.Pinel, J.Laskar, and E.M.Tentzeris, "A Compact LTCC-based Ku-band Transmitter Module," *IEEE Transactions on Advanced Packaging*, Vol.25, No.3, pp.374-384, Aug. 2002.

[4] B.G.Choi, M.G.Stubbs, and C.S.Park, "A Ka-Band Narrow Bandpass Filter Using LTCC Technology," *IEEE Microwave and Wireless Components Letters,* Vol.13, No.9, pp. 388-389, Sep. 2003.

[5] V.Piatnitsa, E. Jakku, and S.Leppaevuori, "Design of a 2-Pole LTCC Filters for Wireless Communications," *IEEE Transactions on Wireless Communications*, Vol.3, No.2, Mar. 2004, pp.379-381.

[6] M.J.Hill, R.W.Ziolkowski, and J.Papapolymerou, "Simulated and Measured Results from a Duroid-Based Planar MBG Cavity Resonator Filter," *IEEE Microwave and Wireless Components Letters,* Vol.10, No.12, pp. 528-530, Dec. 2000.

[7] H.-J.Hsu, M.J.Hill, J.Papapolymerou, and R.W.Ziolkowski, "A Planar X-Band Electromagnetics Band-Gap (EBG) 3-Pole Filter," *IEEE Microwave and Wireless Components Letters,* Vol.12, No.7, pp. 255-257, July 2002.

[8] C.A.Tavernier, R.M.Henderson, and J.Papapolymerou, "A Reduced-Size Silicon Micromachined High-Q Resonator at 5.7 GHz," *IEEE Transaction on Microwave Theory and Technique*, Vol. 50, NO. 10, pp. 2305-2314, Oct. 2002.

[9] A.El-Tager, J.Bray, and L.Roy, "High-Q LTCC Resonators For Millimeter Wave Applications," in *2003 IEEE MTT-S Int. Microwave Sym. Dig*, Philadelphia, PA., June 2003, pp. 2257-2260.

[10] P.Ferrand, D.Baillargeat, S.Verdeyme, J.Puech, M.Lahti, and T.Jaakola, "LTCC reduced-size bandpass filters based on capacitively loaded cavities for Q band application," in *2005 IEEE MTT-S Int. Microwave Sym. Dig*, Long Beach, CA., June 2005, pp. 1789-1792

[11] X.Gong, W.J.Chappell, and L.P.B.Katehi, "Multifunctional Substrates For High-Frequency Applications," *IEEE Microwave and Wireless Components Letters,* Vol.13, No.10, pp. 428-430, Oct. 2003.

[12] M.Ito, K.Maruhashi, K.Ikuina, T.Hashiguchi, S.Iwanaga, and K.Ohata, "60-GHz-band Dielectric Waveguide Filters with Cross-coupling for Flip-chip Modules," in *2002 IEEE MTT-S Int. Microwave Sym. Dig*, Seattle, WA., June 2002, pp. 1789-1792.

[13] S.T.Choi, K.S.Yang, K.Tokuda, and Y.H.Kim, "A V-band Planar Narrow Bandpass Filter Using a New Type Integrated Waveguide Transition," *IEEE Microwave and Wireless Components Letters,* Vol.14, No.12, pp. 545-547, Dec. 2004.

[14] M.Chatras, P.Blondy, D.Cros, O.Vendier, C.Drevon, and J.L.Cazaux, "Narrow Band Micro-Machined Band Pass Filter and A Surface-Mountable Topology," in *Proc. 33rd European Microwave Conference*, Munich, Germany, Oct. 2003, pp. 813-815.

[15] T.Euler and J.Papapolymerou, "Slicon Micromachined EBG Resonator and Two-Pole Filter with Improved Performance Characteristics," *IEEE Microwave and Wireless Components Letters,* Vol.13, No.9, pp. 373-375, Sep. 2003.

[16] Robert E. Collin, *Foundations for Microwave Engineering*, New York, NY/U.S.A: McGraw Hill, 1992.

[17] Y. Cassivi and K.Wu, "Low Cost Microwave Oscillator Using Substrate Integrated Waveguide Cavity," *IEEE Microwave and Wireless Components Letters,* Vol.13, No.2, pp. 48-50, Feb. 2003.

[18] D.M.Pozar, Microwave Engineering, 2nd ed. New York:Wiley, 1998.

[19] D.M.Pozar and D.H.Schaubert , *Microstrip Antennas*, New York, NY/ U.S.A: IEEE press, 1995.

[20] H.Wheeler, "Coupling Holes Between Resonant Cavities or Waveguides Evaluation In Terms of Volume Ratios," *IEEE Transaction on Microwave Theory and Technique*, vol. MTT-12, pp. 231-244, Mar. 1964.

[21] W.H.Leighton and A.G.Milnes, "Junction Reactance and Dimensional Tolerance Effects on X-band 3 dB Directional Couplers," *IEEE Transaction on Microwave Theory and Technique*, vol. MTT-19, pp. 818-824, Oct. 1971.

[22] J.-S. Hong and M.J.Lancaster, *Microstrip Filters for RF/Microwave Applications*, New York, NY/U.S.A: John Wiley & Sons, Inc., 2001.